NASA TECHNICAL MEMORANDUM

NASA TM X-1753

NASA TM X-1753

AMPTIAC

PRELIMINARY DEVELOPMENT OF SPECTROCHEMICAL ANALYSIS OF SUPERALLOYS WITH THE LIQUID-LAYER SOLID-SAMPLE SPARK TECHNIQUE

by Ramon M. Barnes

Lewis Research Center
Cleveland, Ohio

NATIONAL AERONAUTICS AND SPACE ADMINISTRATION • WASHINGTON, D. C. • MARCH 1969

NASA TM X-1753

PRELIMINARY DEVELOPMENT OF SPECTROCHEMICAL ANALYSIS OF SUPERALLOYS WITH THE LIQUID-LAYER SOLID-SAMPLE SPARK TECHNIQUE

By Ramon M. Barnes

Lewis Research Center
Cleveland, Ohio

NATIONAL AERONAUTICS AND SPACE ADMINISTRATION

For sale by the Clearinghouse for Federal Scientific and Technical Information
Springfield, Virginia 22151 – CFSTI p[redacted]

ABSTRACT

A comparison study is made, for the spectrochemical analysis of cobalt-base superalloys, between the liquid-layer solid-sample spark technique and the conventional point-to-plane spark analysis in air. The changes of analytical concentration curves are indicated for alloying constituents of two developmental cobalt-base alloys, and correlation of the changes to preliminary microscopic, metallographic, and spectroscopic phenomena are hypothesized.

PRELIMINARY DEVELOPMENT OF SPECTROCHEMICAL ANALYSIS OF SUPERALLOYS WITH THE LIQUID-LAYER SOLID-SAMPLE SPARK TECHNIQUE

by Ramon M. Barnes

Lewis Research Center

SUMMARY

The liquid-layer solid-sample spark technique was compared with conventional point-to-plane spark analysis for developmental cobalt-base superalloys during further development of a spark spectroanalytical method. The comparison indicated an apparent reduction of matrix effects for several elements when the liquid-layer solid-sample spark technique was employed. However, preliminary examination of the samples and the spectra indicated the possibility that a number of complex phenomena combine to appear as the matrix-effect reduction.

A supplementary spark material transfer technique with direct-current arc excitation was accurate in producing results consistent with the spark transfer process for spectrochemical analysis of cobalt-base superalloys.

INTRODUCTION

The results of previous experiments with the liquid-layer solid-sample spark technique using a conventional spark source indicated that spark analysis of refractory alloys and superalloys may be feasible by that method (ref. 1). The liquid-layer solid-sample spark technique (hereinafter called the liquid-layer spark technique) requires that a layer of liquid be moved across the flat surface of a solid sample while a spark discharge is passed between sample and counterelectrodes. Conventional point-to-plane spark analysis is similar experimentally to the liquid-layer spark technique without the application of a liquid layer.

Earlier observations with the liquid-layer spark technique indicated an increase in amount of sample material removed, an increase in signal-to-background ratio for selected lines, and a potential elimination of sampling interactions compared with conventional point-to-plane spark analysis (ref. 1). The present study was undertaken to

investigate the applicability of this technique to spectrochemical analysis of chromium-, cobalt-, and nickel-base superalloys, because no standard spark analysis methods were available (ref. 2). The preliminary results reported herein refer only to studies conducted with developmental cobalt-base superalloys, although some experimental parameters were established with aluminum alloys.

A second spectrochemical method for the analysis of superalloys was tested concurrently. In this method, the sample material deposited on the graphite counter-electrode during sparking was subsequently analyzed with a direct-current arc.

EXPERIMENTAL

In the present investigation with the liquid-layer spark technique, operating equipment was the same as reported previously (ref. 1). The spark operating conditions are given in table I.

A new sample-holding device was fabricated and employed, as illustrated in figure 1. This device eliminated the aspirator support rod described previously in including an aspirator mount as a part of the stand. This reduced the difficulty in reproducibly positioning the aspirator. Like the previous sample holder, this device was made of chemically resistant plastic and permitted unhindered solution flow on the electrode surface as well as an uninterrupted optical path in two directions.

The effects of the flow rate of the aspirating gas and the flow rate of the liquid were studied to determine optimum operating conditions. This study is described in the appendix. For the analyses reported here, a 0.5-millimeter inside-diameter aspirator operating at an air flow rate of 7670 cubic centimeters per minute was used with a pumped liquid flow rate of approximately 2.5 cubic centimeters per minute.

For the preliminary development of spark spectroanalysis of superalloys, water and aqueous solutions were used in the liquid-layer spark technique. The effect of dielectric liquids on spark results is also discussed in the appendix.

TABLE I. - SPARK OPERATING CONDITIONS

Parameter	Condition 1	Condition 2
Resistance, ohm	Residual	Residual
Inductance, μH	Residual	Residual
Capacitance, μF	0.010	0.015
Discharge voltage, V	17 000	17 000
Discharges per cycle	4	4
Radiofrequency current, A	15	20

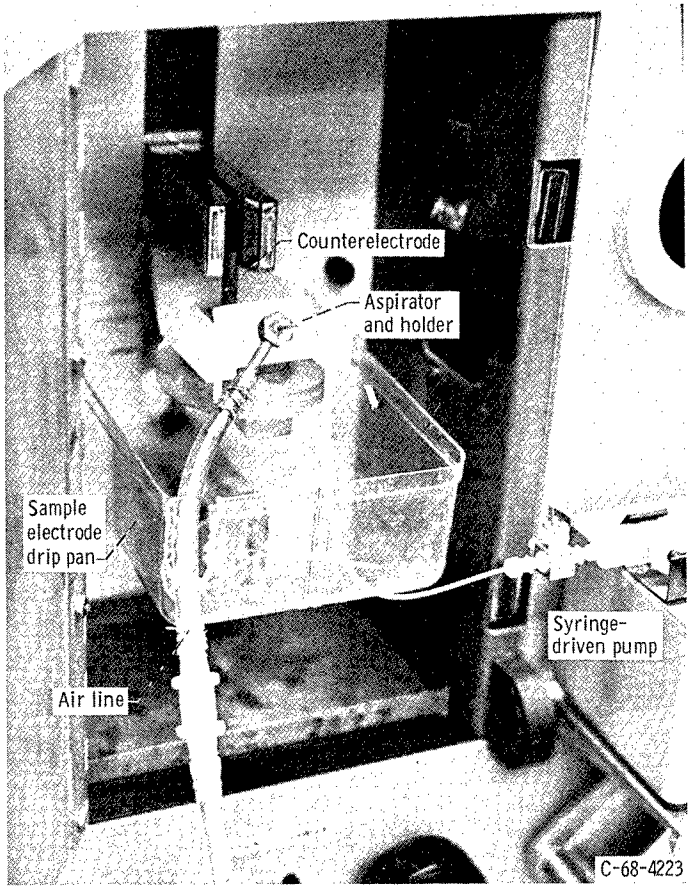

Figure 1. - Apparatus for applying liquid layer on solid sample.

RESULTS AND DISCUSSION

Spark Analysis of Superalloys

Previous observations of nickel and cobalt alloys indicated that an increase in line-to-background ratio could be obtained when a liquid layer was applied to the sample surface during sparking. The present study reports the improvement of a spark method for developmental cobalt-base superalloys when the liquid-layer spark method is used in place of conventional point-to-plane analysis.

For this investigation, two developmental cast cobalt-base alloy groups, for which independent chemical analyses had been made, were available. Tests were performed on four chemically analyzed specimens of one alloy group (group A) and three of the second group (group B). The chemical analysis ranges are given in table II. The compositions of specimens within both group A and group B alloys had been intentionally varied in previous metallurgical studies. Two commercial cobalt-base superalloys were

TABLE II. - APPROXIMATE CHEMICAL ANALYSIS

Element	Alloys			
	Group A	Group B	S816	L605
	Composition, wt. %			
Aluminum	0	6 to 7	0.02	0
Chromium	1 to 3	1 to 3	19	20
Cobalt	66 (Bal.)	37 (Bal.)	52 (Bal.)	43
Iron, rhenium	2 to 6	0	3	0
Nickel	1 to 3	37	20	10
Titanium	0.5 to 1.0	0.5 to 1.7	0	0
Tungsten	17 to 20	13	4	15
Zirconium	0.3 to 0.6	0.3 to 0.6	0	0

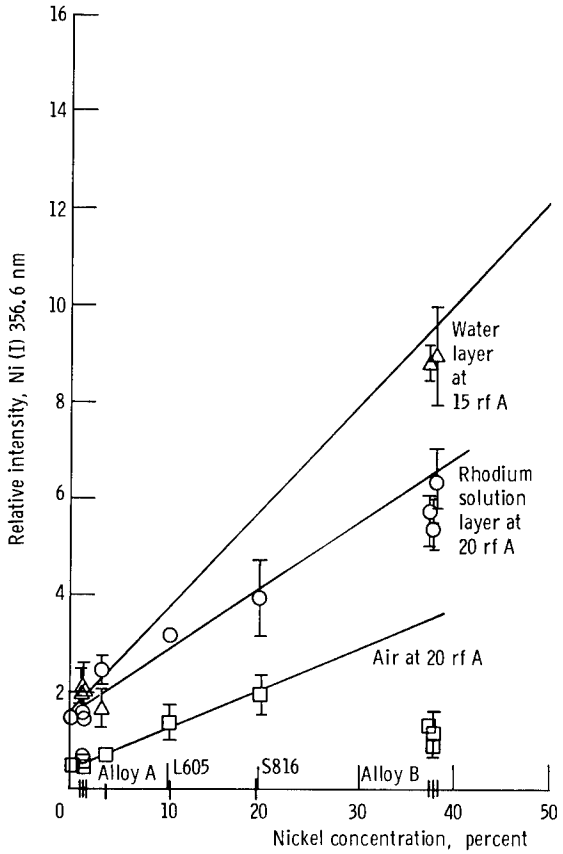

Figure 2. - Analytical concentration curve for nickel in air and with rhodium-solution-layer spark technique and water-layer spark technique.

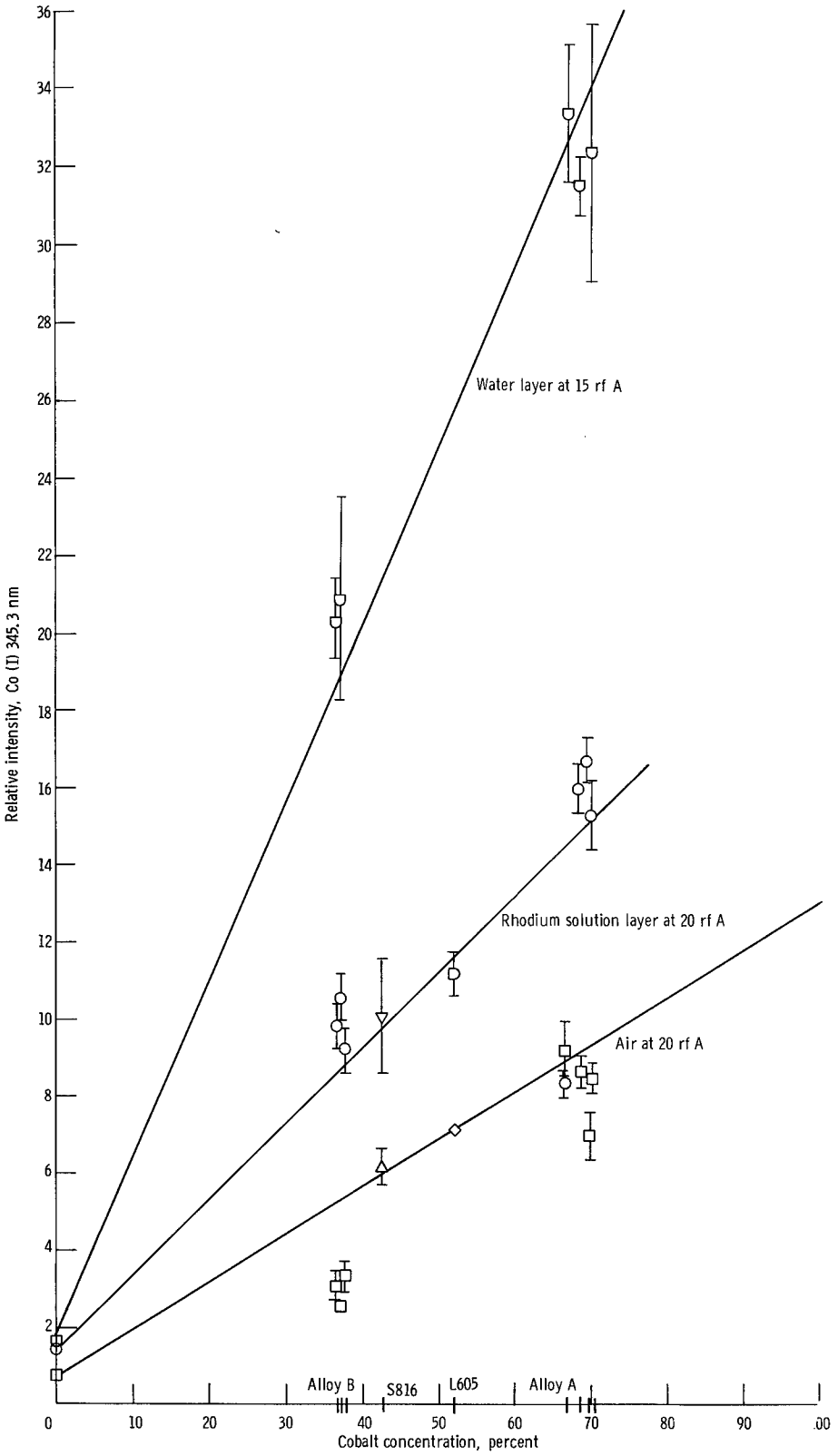

Figure 3. - Analytical concentration curve for cobalt in air, with rhodium-solution-layer spark technique and water-layer spark technique.

also included in the study, and their compositions are given in table II.

After spark analysis with and without the liquid-layer spark technique, the readout signal corrected for blank and background was plotted as a function of the element concentrations for all elements in table II. Titanium, zirconium, chromium, and tungsten were given special attention, because they were contained in similar concentration levels in both alloy groups. When the results were compared with and without the liquid-layer spark technique, the line intensities were nearly always greater with the liquid-layer spark technique.

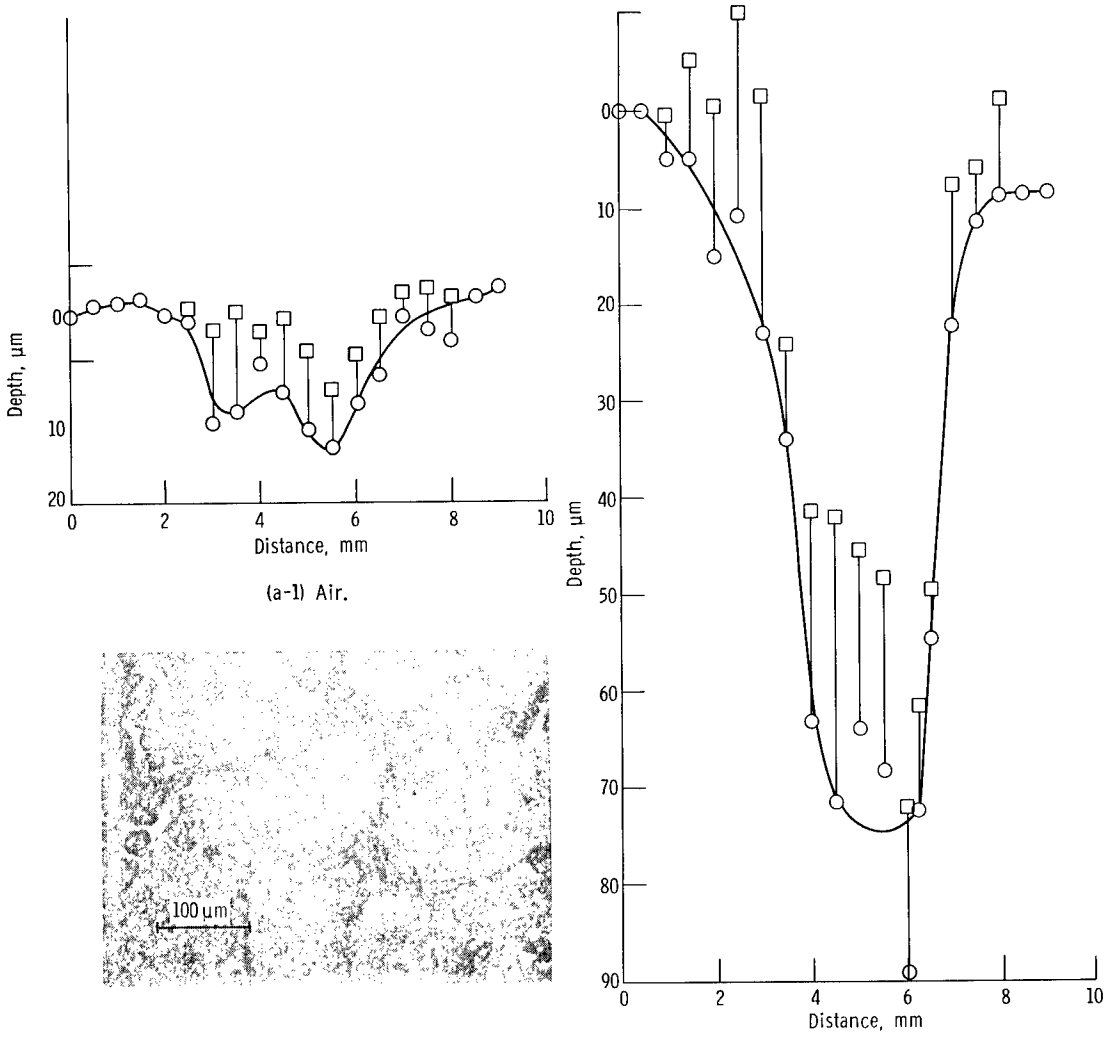

(a) Alloy group A.

Figure 4. - Crater profiles for alloy A and B samples with and without water-layer spark technique. Profiles drawn through average of crater low points. Spark time, 70 seconds; radiofrequency current, 15 amperes.

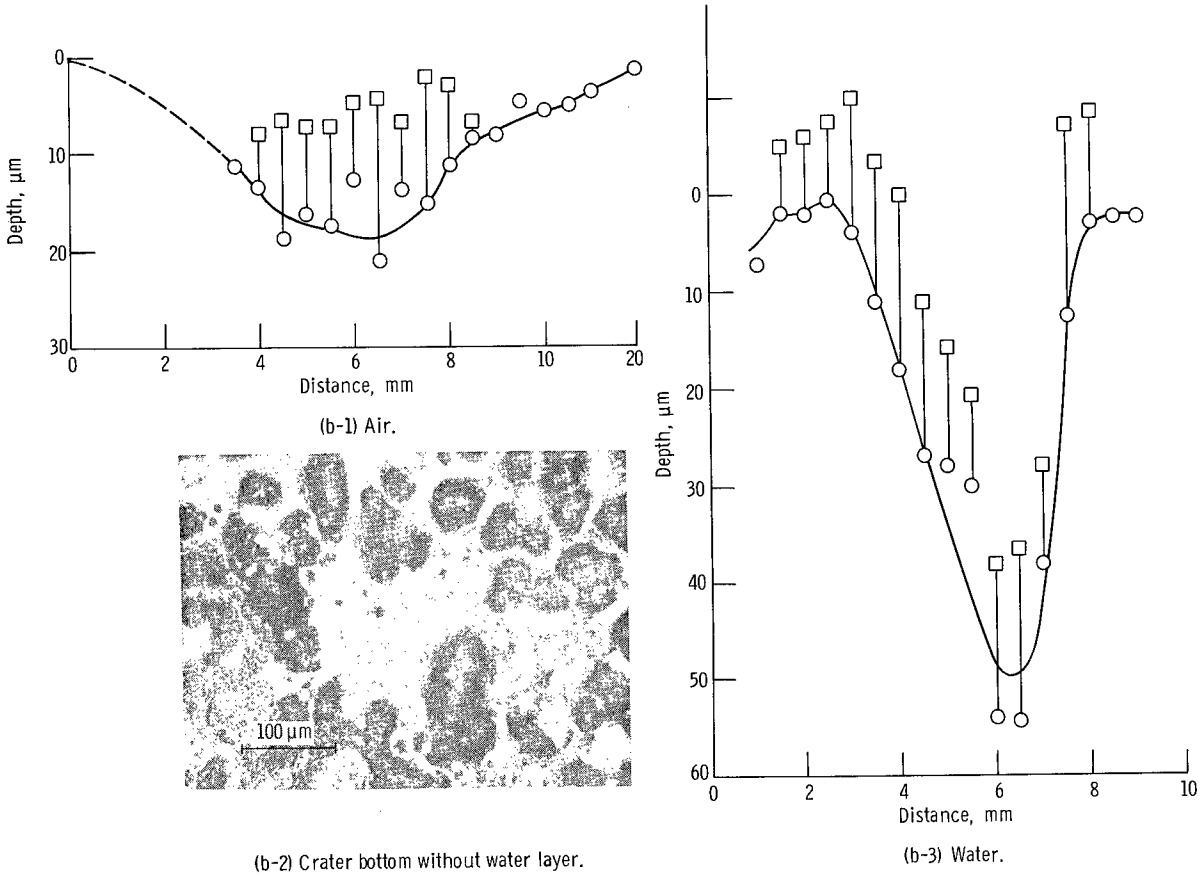

(b-1) Air.

(b-2) Crater bottom without water layer.

(b-3) Water.

(b) Alloy group B.

Figure 4. - Concluded.

Nickel and cobalt intensities were also considered. The response for sparking in air with a 0.3 percent rhodium nitrate solution layer (at spark condition 1), and with a water layer (at spark condition 2) is given for nickel in figure 2 and for cobalt in figure 3. The two additional intensity values correspond to cobalt and nickel concentrations in the commercial cobalt-base superalloys. In both examples, the slope of the curves with the liquid-layer spark technique is greater than that observed for sparking in air. Additionally, the nickel and cobalt intensities for the samples from group B alloys in air fall below the line drawn through the intensities for the commercial alloys and the group A alloys. However, when the liquid-layer spark technique was used with the same alloys, each set of data fitted a single line. Similar observations were made for neutral atom emission for chromium 425.4 nanometers (4254 Å) and tungsten 400.8 nanometers (4008 Å) at both spark conditions.

The increase in curve slope and reduction of differences between alloy group A and B intensities may result from two interdependent effects. The first is the effect of the amount of sample removed from the electrode specimen: as more material is

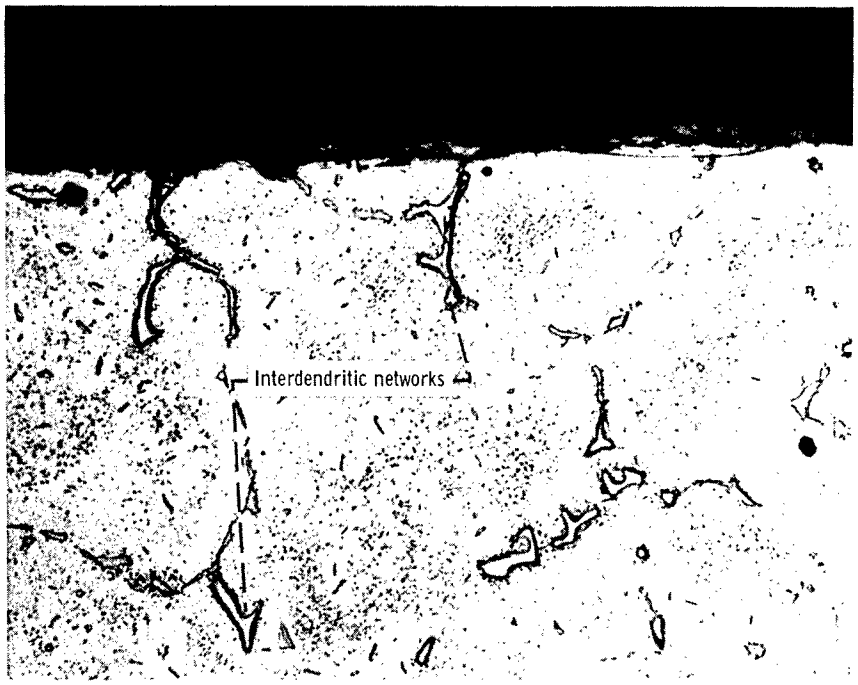

(a) Alloy A; sparked in air.

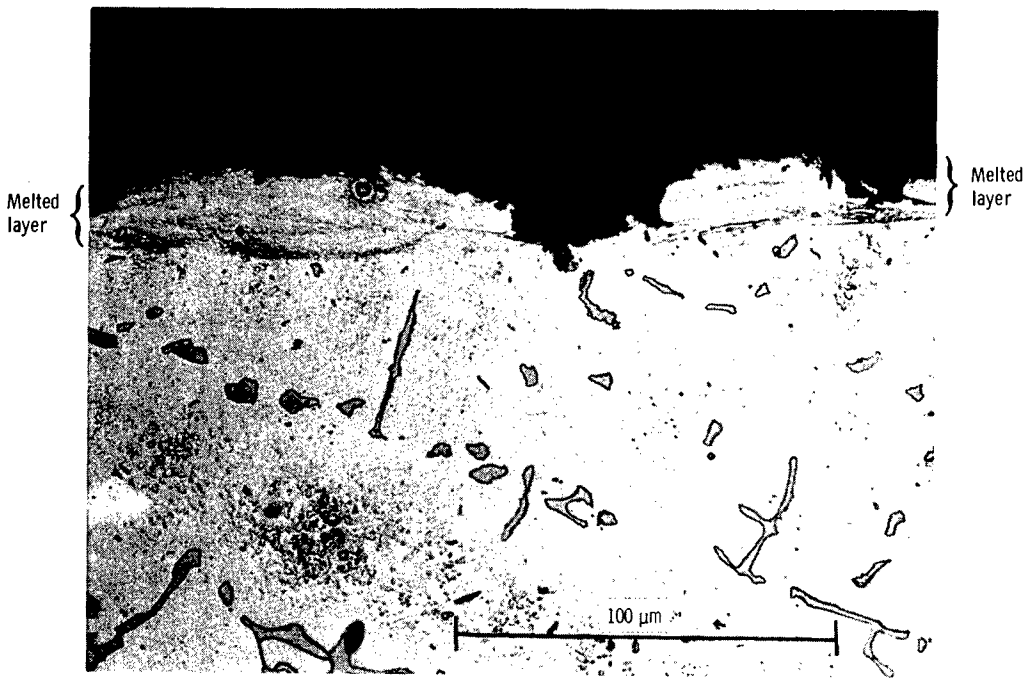

(b) Alloy A; sparked with water layer. C-68-4221

Figure 5. - Sections of spark craters. Spark time, 15 seconds; radiofrequency current, 15 amperes.

(c) Alloy B; sparked in air.

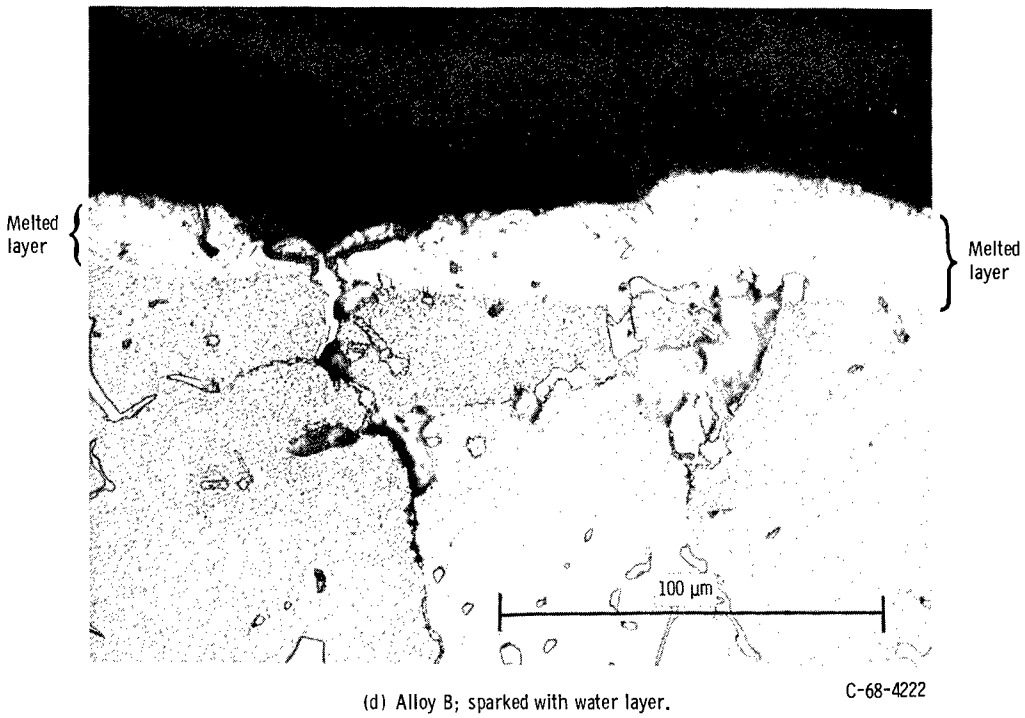

(d) Alloy B; sparked with water layer.

Figure 5. - Concluded.

removed into the spark, the spectral emission is expected to increase in proportion. The second is an increase in neutral atom line intensity and a decrease of ion line intensity with the liquid-layer spark technique (ref. 1).

In determining the influence of amount of sample removed, differences in spark-sample interactions were detected between the two alloy groups by direct metallographic examination of the spark craters and of polished sections through the spark craters. Samples were prepared for both alloy groups with and without the water-layer spark technique. Micrographs of craters made with and without a water layer are shown in figure 4 as are spark crater profiles determined from optical microscopic examination. The peak and valley portions of the crater contour are indicated. The crater profiles are estimated from the values and visual observations. Photomicrographs (×500) of the crater cross sections for a 15-second spark (condition 1) are presented in figure 5.

The sample of alloy group A appears to have more material removed in air than does the sample of alloy group B. The B group sample also appeared to have undergone more melting in air than the A group sample as observed visually and from the appearance of a melted layer in the photomicrograph cross section. This apparent melting and sampling may reflect a lower melting point in the alloy group B sample than in the alloy group A sample.

The crater of the alloy group A sample in figure 4 appears to show preferential melting of interdendritic regions when sparked in air. Generally, the interdendritic material has a lower melting point than the adjacent area, because it is the last composition to solidify. In the sample from alloy group A, the interdendritic material tends to contain metal carbides (ref. 3). The difference in crater profiles for group A sample and group B sample in air may be the result of a lower bulk melting point of group B alloy and the preferential melting of interdendritic carbide networks of the group A sample.

With the water-layer spark technique, both samples show an increase in spark crater volume, surface irregularities, and distinctive melted layers. The spark crater is larger for the group A sample than for the group B sample. No indication of preferential melting of an interdendritic network could be detected in the group B sample crater from either visual microscopic or photomicrographic examination. The melted layer of the spark crater accounts for the shiny appearance of the crater to the eye.

The increase in crater volume produced by the liquid-layer spark technique was greater for the group A sample than for the group B sample. This result could not have been predicted and may be related to the bulk melting points and the thermal conductivities of the alloys.

The indications obtained for the difference in apparent material removal between the two alloy group samples are not consistent with the relative positions of nickel and cobalt intensities on the curves of figures 2 and 3. For example, the group B alloy

intensities for both nickel and cobalt in air are lower than the concentration curve, although the group B alloy sample apparently underwent more melting and had more sample removed than alloy group A sample. Also, the increase in nickel and cobalt intensities with the liquid-layer spark technique is not completely reflected by the changes in spark crater volume. Although group A alloy sample showed a larger increase in sample removal than the group B sample, the intensity increase for both nickel and cobalt values of group B were greater than those of group A. This apparent lack of correlation emphasizes the possibility of the second controlling effect, that is, the increase of neutral atom emission with the liquid-layer spark technique. The increase in neutral atom emission from group B alloys may be sufficient to give a response proportional to the other alloy samples with the liquid-layer spark technique and may account for the nickel, cobalt, tungsten, and chromium results.

The behavior of concentration responses for titanium and zirconium in alloy groups A and B obtained with and without the liquid-layer spark technique was substantially different from the behavior described for nickel, cobalt, chromium, and tungsten. Figure 6 shows the analytical concentration curves for titanium with and without the application of a 0.3 percent rhodium solution layer to alloy groups A and B at spark condition 2. Under both situations, the alloy A and B samples result in two concentration curves. The curves for alloy group A show greater intensities than the curves for alloy group B. Although the alloy B sample had a larger spark crater in air, the greater intensity for alloy group A in air might reflect the preferential sampling of the interdendritic carbide network in alloy group A. The large increase in slope of the curves for group A alloy samples with the liquid-layer spark technique is consistent with the increase in spark crater dimension of figure 4. The curves for group B samples, on the other hand, show a much less pronounced increase in slope, which may be explained partly by the smaller change in spark crater size for this alloy group than for group A. This behavior may also be related to the actual removal of the titanium carbides in the alloys but was not pursued in this investigation.

The analytical concentration curves for zirconium with and without the liquid-layer spark technique are given in figure 7. Two curves are obtained for spark analysis in air at the two spark conditions. (Spark condition 2 results are not presented in fig. 7.) However, the response for zirconium concentration changes in alloy group B is greater than for alloy group A. This response is opposite that observed for titanium concentrations in figure 6. Preferential sampling of the interdendritic carbide network in group A alloys, which should be richer in titanium carbide than zirconium carbide, may be the reason for this result. In contrast, the sampling in group B alloys appeared more uniform over the entire crater, and no preference for interdendritic carbides was detected visually or photomicroscopically.

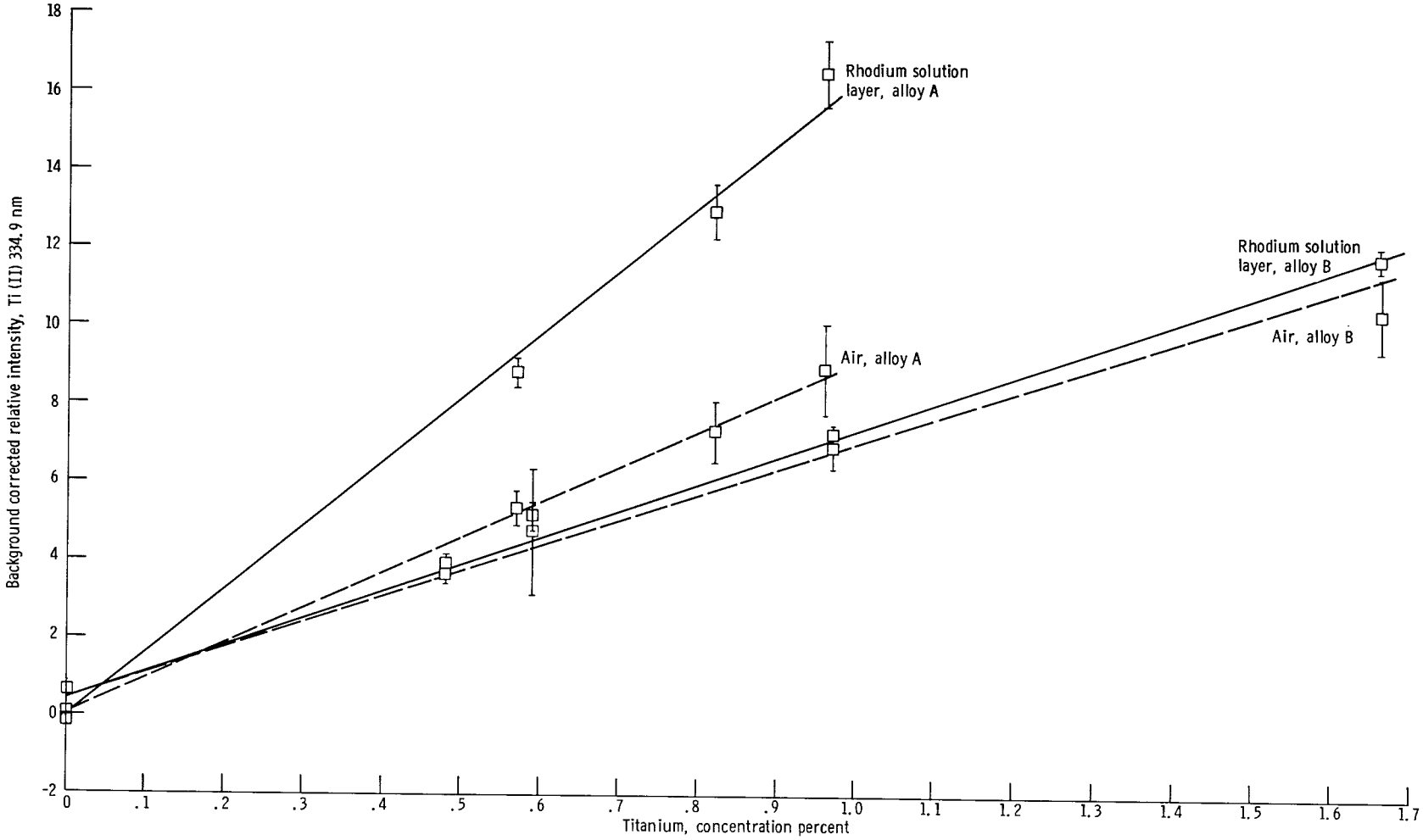

Figure 6. - Titanium analytical concentration curves for alloy groups A and B with and without rhodium-solution-layer spark technique. Spark condition 2 (see table I); exposure, 20 seconds.

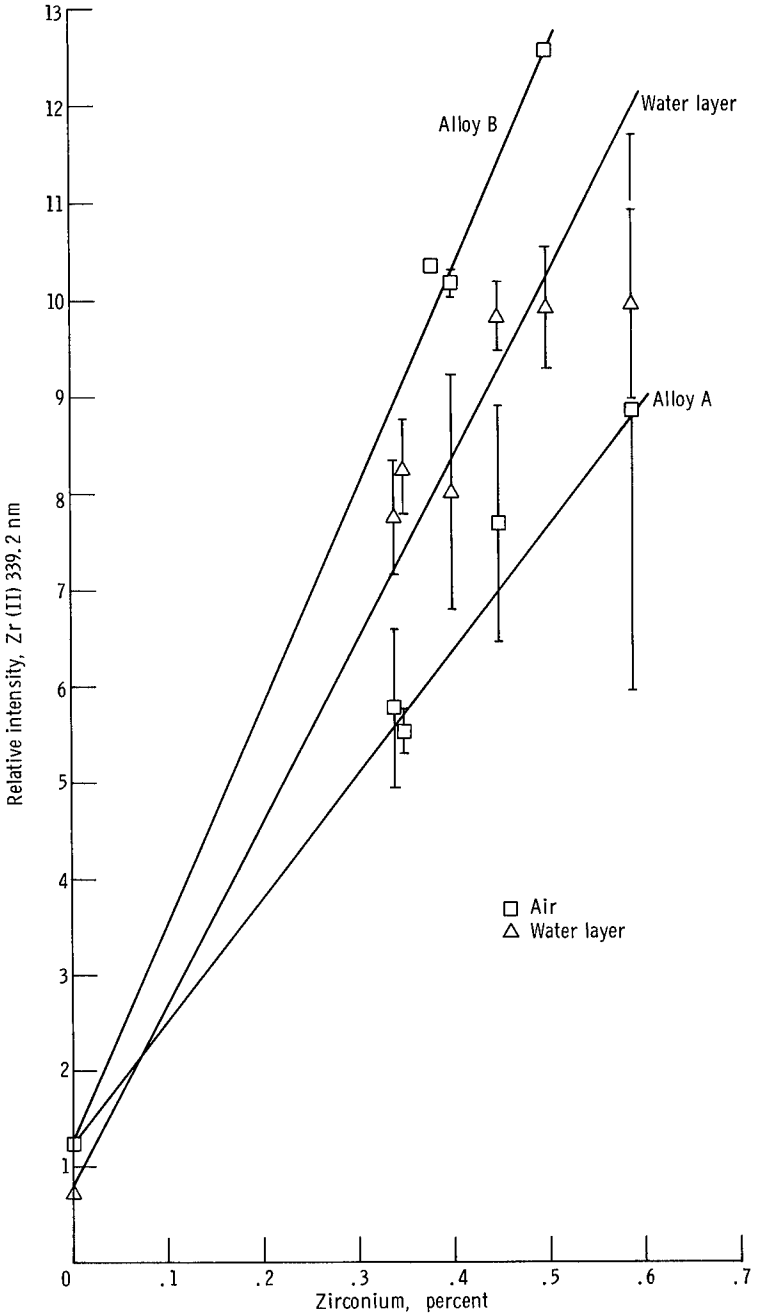

Figure 7. - Zirconium analytical concentration curves for alloy groups A and B with and without water-layer spark technique. Spark condition 1 (see table I); exposure, 20 seconds.

The zirconium intensities for alloy group A increased with the liquid-layer spark technique. More sample was taken over the entire spark crater than when sparked in air. Because the zirconium carbide distribution in the alloy might possibly be different from the titanium carbide distribution (as it is in alloy group B), an improved representation of the zirconium concentration could be expected as more sample is taken. In contrast, the zirconium intensities for alloy group B dropped. When a water-layer spark technique (spark condition 1) or a rhodium-solution-layer spark technique (spark condition 2) was used, the zirconium intensities from both alloy groups formed a single line almost within the precision range (as indicated by the 95 percent confidence limits) of individual data points. The decrease in alloy group B zirconium response may be the result of the relative decrease in zirconium ion emission with the liquid-layer spark technique. For alloy group A intensities, this decrease may be offset by the greater amount of sample removed. Thus, what appears to be a reduction of matrix effect in the apparent merging of two curves, may be a fortuitous balance of other interactions.

Further studies of the distribution of elements in the alloys and the relative neutral atom and ion emission intensities are required to confirm these suggested explanations.

Direct Current Arc Analysis of Counterelectrode Deposits

The material deposited on the graphite counterelectrode during spark analysis can be used as the sample for further analysis in the direct-current arc. This spark material transfer technique was studied concurrently with the spark investigation of superalloys as an alternate spectrochemical method. This method may permit the preparation of samples on counterelectrodes which can be used in place of the spark analysis to take advantage of the common sample form, the addition of an internal standard, and the high sensitivity of the direct-current arc.

The results for titanium in the direct-current arc analysis of counterelectrode deposits from the spark transfer analysis of cobalt-base superalloys of figure 6 are given by the analytical concentration curves in figure 8. Each alloy group results in two distinct concentration curves. The values in air are not well resolved by the scale in figure 8. The difference between samples prepared with and without the liquid-layer spark technique is pronounced. The direct relation between the spark and arc intensities is further demonstrated in a plot of arc intensities as a function of spark intensities in figure 9. The results of the arc analysis are directly proportional to the results of the spark analysis. The displacement of the curves is related to the difference in sensitivity observed for different sparking techniques. The greatest difference is observed between spark transfer in air and spark transfer with the liquid-layer spark technique. Figure 9 also gives the 95 percent confidence limits of individual data points for the two

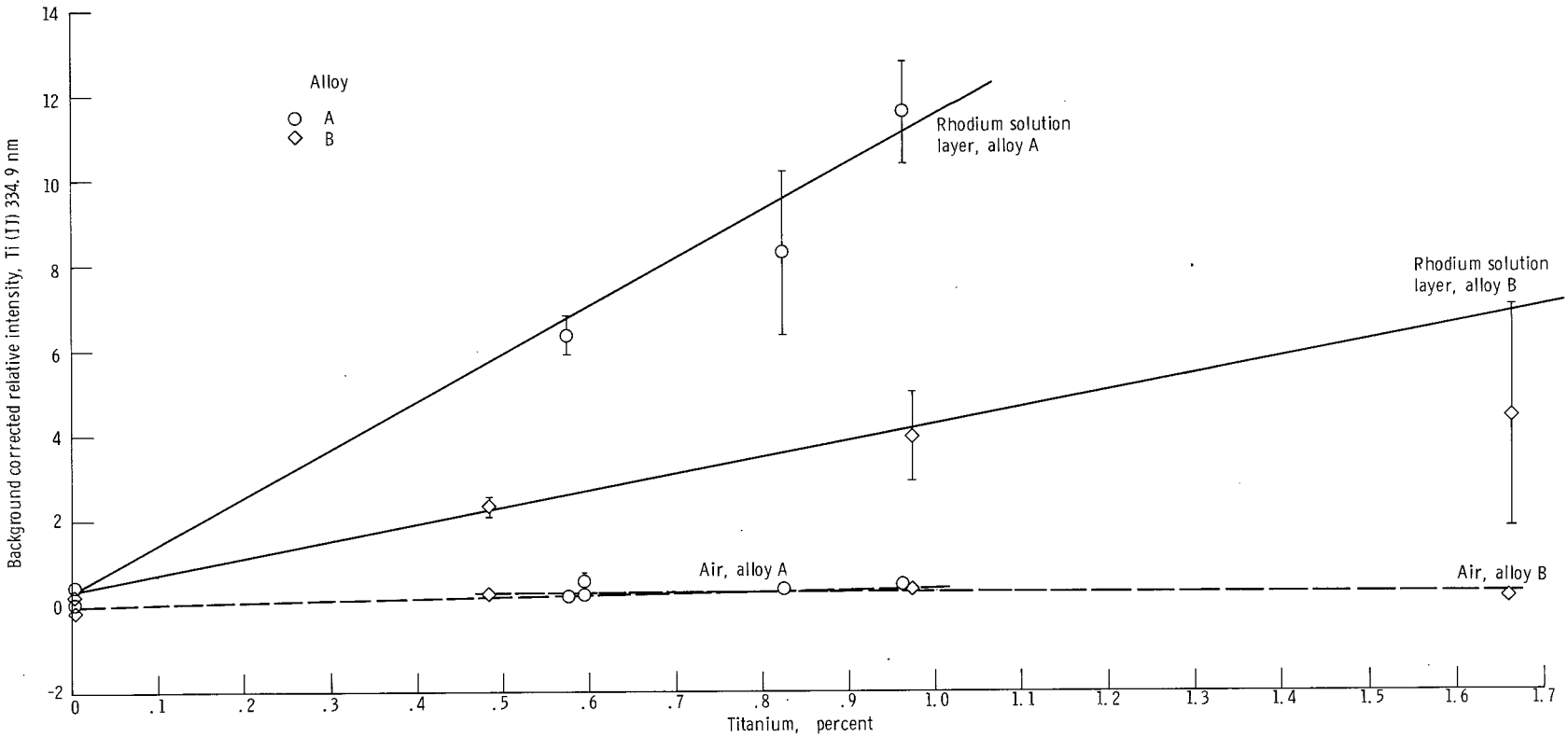

Figure 8. - Titanium analytical concentration curves for direct-current arc analysis of spark material transfer samples. Current, 13 amperes; exposure, 20 seconds.

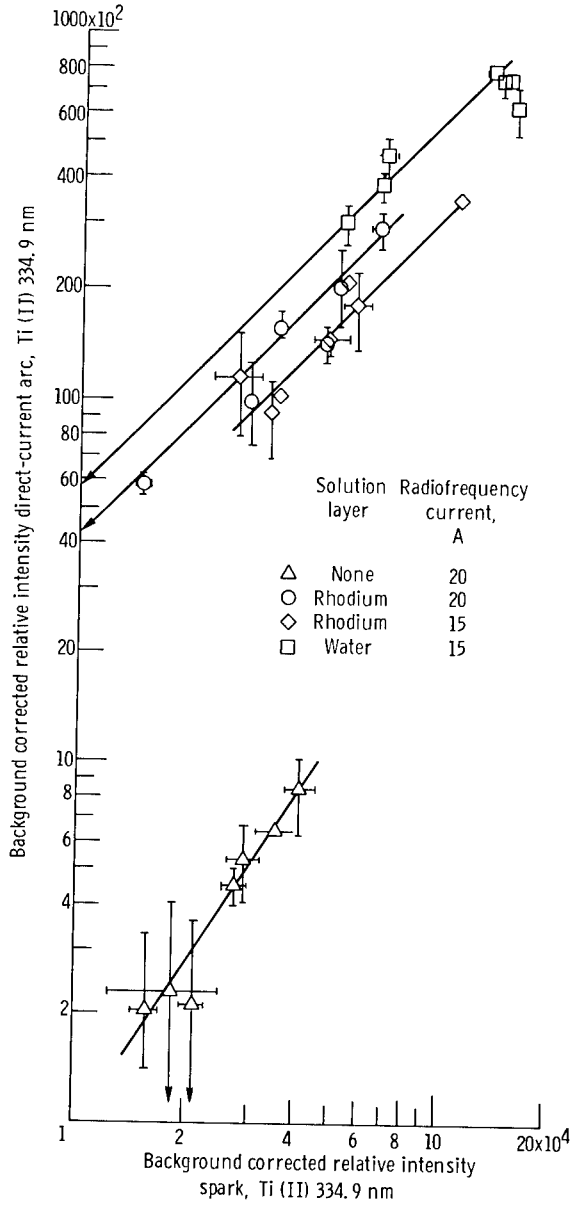

Figure 9. - Correlation of titanium intensities for direct-current arc analysis and spark analysis.

analytical methods. In most of the examples, the precision of the spark analysis is better than the precision of the arc method. However, the precision of the arc results is directly dependent upon the precision of the spark transfer process.

The titanium results of figure 8 further verify the interpretation of figure 6. The increase in titanium response with and without the liquid-layer spark technique appears to be largely the result of differences in the amount of sample removed. The low response for alloy groups A and B in air in figure 8 results from the small amount of material collected on the graphite counterelectrode during the 20-second spark sampling in air. The increase in alloy group A sample signal intensity is greater than the increase in alloy group B sample signal intensity corresponding to the greater increase in sample removed from alloy group A.

The sensitivity of the method is increased by increasing the amount of material transferred to the counterelectrode. By increasing the spark transfer time, more material can collect up to a limit. Ideally, the high-current, unipolarity, oscillatory spark described in reference 4 should be used for building a deposit on the counter-electrode to obtain the desired sensitivity. This source is desirable because the counterelectrode does not become the sample electrode on alternate current half cycles of the spark discharge.

The results of the spark transfer with the rhodium-solution-layer spark technique indicated that internal standard ratios to rhodium were more effective in correcting run-to-run deviations for most elements than were nickel or cobalt internal standards.

The difficulties inherent in the direct-current arc remain with the material transfer technique. For example, tungsten was transferred in proportion to increasing tungsten concentrations from an alloy surface by the liquid-layer spark technique. In the direct-current arc analysis in air, as the electrode was heated by the arc, the high tungsten concentration samples were converted on the electrode from the deposit to refractory tungsten compounds. These refractory tungsten compounds were not then quantitatively removed from the electrode during the arc exposure.

CONCLUDING REMARKS

The development of spark spectrochemical analysis for cobalt-base superalloys with the liquid-layer spark technique has given preliminary results for two developmental alloy groups, which indicated the feasibility of the analysis. However, the apparent reduction of matrix effects observed for chromium, cobalt, nickel, tungsten, and zirconium may be the result of fortuitous balancing of a number of complex interactions at the spark-sample electrode surface and in the spark channel. This preliminary investigation has revealed the possible presence of selective sampling of interdendritic

carbide networks in the conventional point-to-plane spark analysis, and the apparent absence of it with the liquid-layer solid-sample spark technique. Processes at the sample electrode and in the spark channel have been hypothesized as a possible rationale for the observations; however, considerable investigation of the sample metallurgy and the spark emission is required before these working hypotheses can be confirmed. Additional experimental data on the physical properties, such as melting point and thermal conductivity, of the alloy groups would aid in further studies. Investigation of the metallurgical distribution of elements and compounds in the alloy should also be completed before an accurate description of the observed phenomena can be made.

The direct-current arc analysis of material transferred to the counterelectrode during spark analysis is accurate in producing results consistent with the spark analysis process and can be used with confidence if the differences in spark transfer amounts can be recognized. The technique is rapid and sensitive and permits the addition of an internal standard from the liquid layer, but it suffers from limitations of the direct-current arc excitation in air, such as compound formation. These limitations may be potentially removed or reduced by other arc excitation procedures.

Lewis Research Center,
National Aeronautics and Space Administration,
Cleveland, Ohio, December 6, 1968,
129-03-14-04-22.

APPENDIX - STUDY AND SELECTION OF OPERATING CONDITIONS FOR THE LIQUID-LAYER SPARK TECHNIQUE

• Aspiration Rate

An earlier study of the effect of the solution flow rate over the solid-sample surface in the liquid-layer spark technique indicated that the amount of material removed and the intensities of selected spectral lines increased with increasing flow rates up to 2.5 cubic centimeters per minute (ref. 1). Ratios of the intensities of spectral lines, however, remained relatively constant for both the material sampled and the solute of the solution layer. In that study, the liquid flow rate was determined by the aspirating gas flow rate

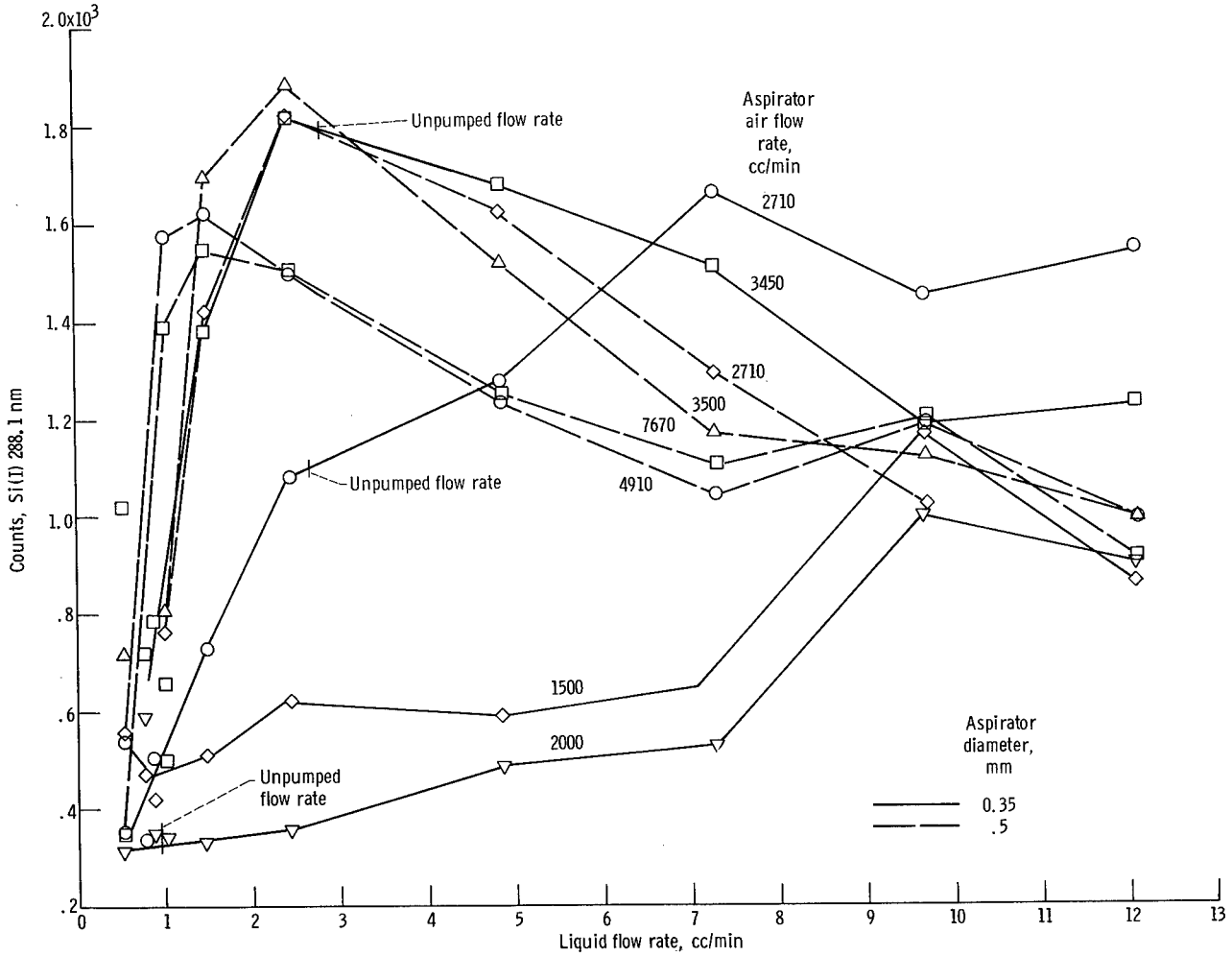

Figure 10. - Silicon spectral response as function of liquid flow rate for different aspirator air flow rates.

through a 0.35-millimeter inside-diameter aspirating nozzle. Two distinct effects are present, however. One is the flow rate of the aspirating gas, and the other is the flow rate of the liquid. In order to distinguish the influence of each of these effects, an experiment is described here in which the flow rates were independently controlled over a large flow rate range. The results of these studies are potentially useful in establishing a description of the spark-sample interaction at the spark site as a function of the liquid flow rate and liquid layer thickness.

Aspirator tubes 0.35 and 0.50 millimeter in inside diameter were used. Flow rates were measured with calibrated rotometers. The sample used was a chill-cast aluminum alloy containing 0.7 percent silicon. A 0.3 percent gallium chloride solution was used, and the solution flow rate was controlled by using a variable-speed, motor-driven syringe pump. Silicon (at 288.1 nm), gallium (at 417.2 nm), and aluminum (at 256.8 nm) intensity values were read and plotted in figures 10 to 12 as a function of solution flow rate. The solution flow rate for the unpumped condition is also indicated for reference.

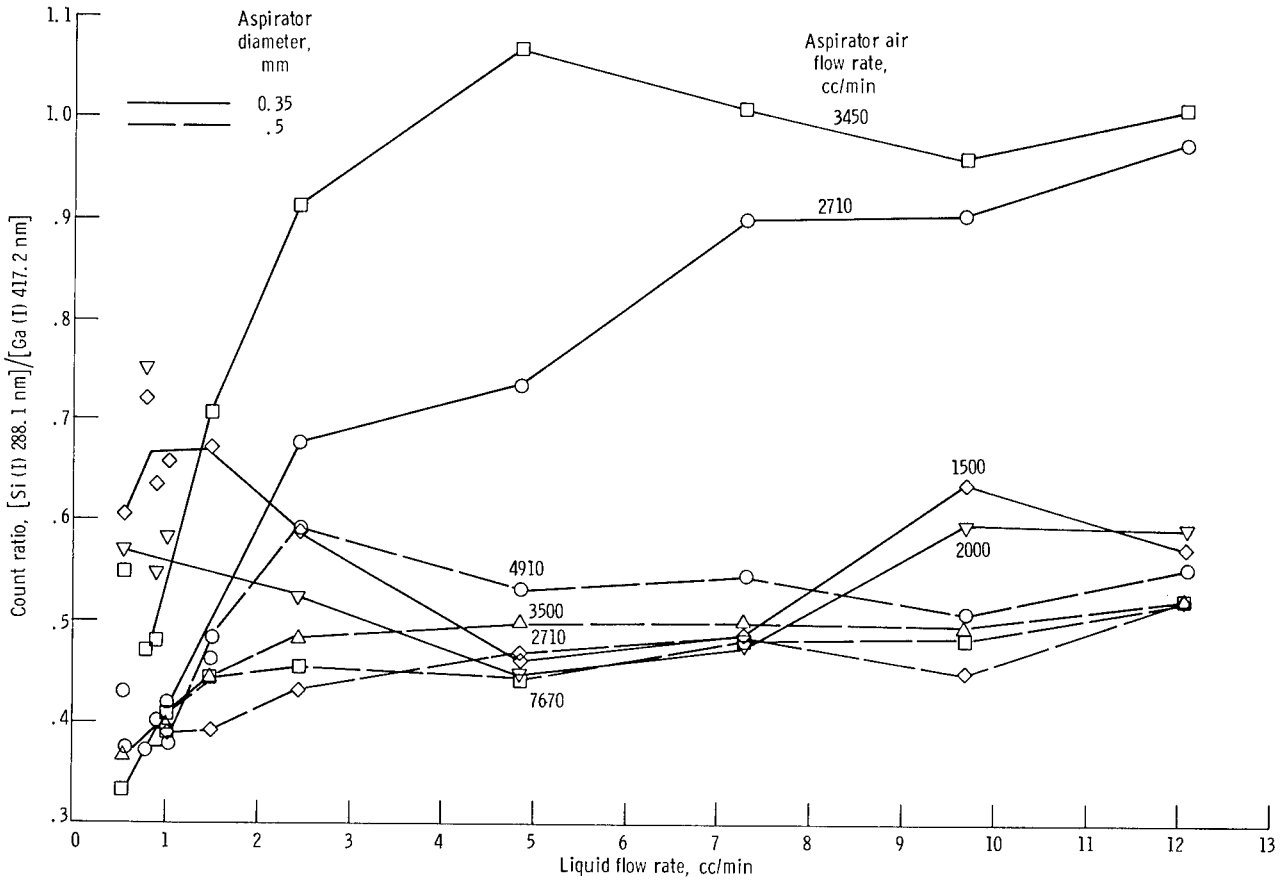

Figure 11. - Spectral response ratio of silicon to aluminum as function of liquid flow rate for different aspiratory air flow rates.

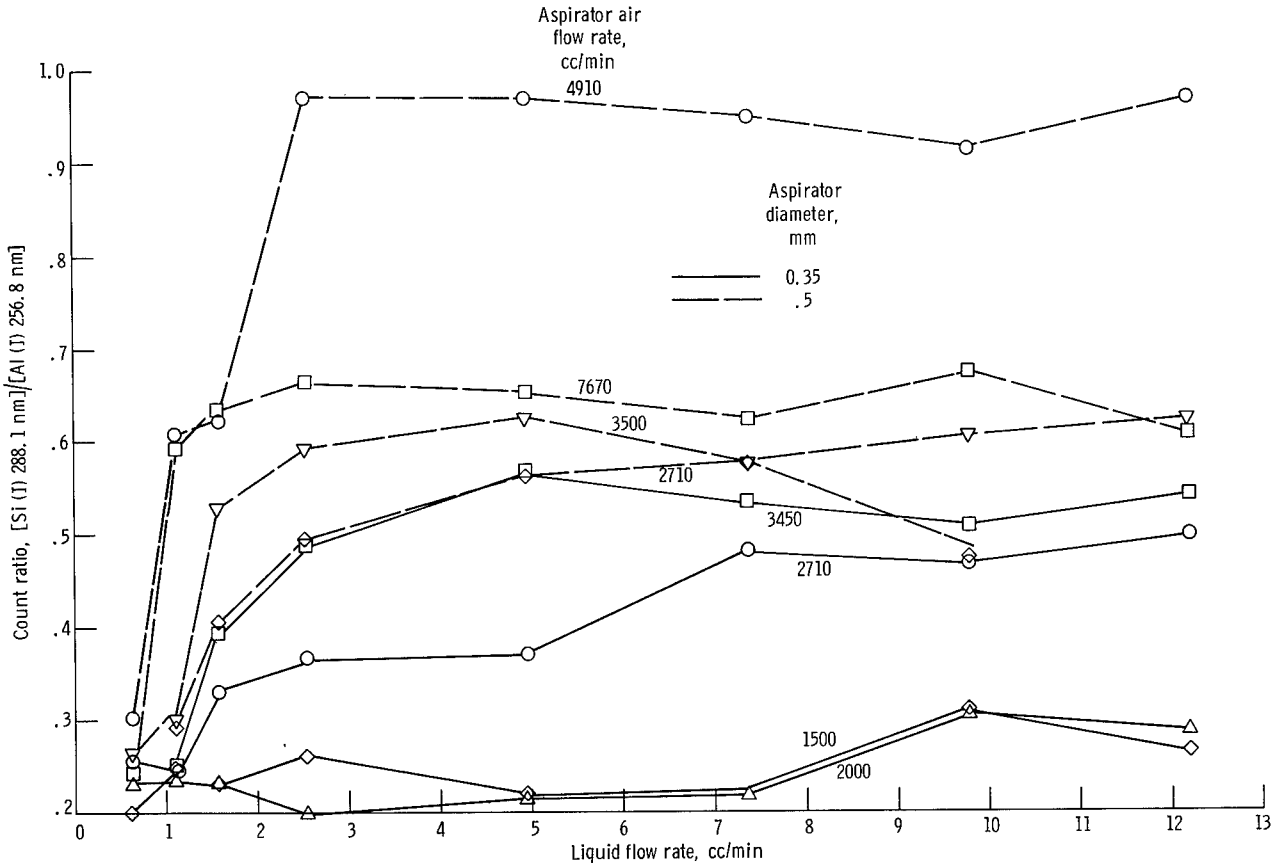

Figure 12. - Spectral response ratio of silicon to gallium as function of liquid flow rate for different aspirator air flow rates.

For the 0.35-millimeter-diameter aspirator, a significant increase in silicon intensity occurred as the air flow rate increased from 1500 to 3450 cubic centimeters per minute. Deep, shiny spark craters, indicating acceptable liquid-layer spark sampling, occurred with a flow rate of 3450 cubic centimeters per minute at solution flow rates greater than 1.0 cubic centimeter per minute. At lower air flow rates, spark craters were generally either completely unacceptable or marginal as the solution flow rate changed. The flow rates from the 0.50-millimeter aspirator were expectedly higher, and the silicon intensities and the spark crater appearance improved over those from the 0.35-millimeter aspirator. As in the eariler study, the silicon intensities with the 0.35-millimeter aspirator increased rapidly as the solution flow rate reached 1 cubic centimeter per minute. In figure 10, a broad peak occurs between 1 and 3 cubic centimeters per minute.

The most consistent ratios observed for silicon to gallium (fig. 11) and silicon to aluminum (fig. 12) occurred for the 0.50-millimeter-diameter aspirator.

For the analysis of superalloys, the optimum conditions observed in this experiment were used: the 0.50-millimeter-diameter aspirator, air flows of 7670 cubic centimeters per minute, and solution flow rates of greater than 1.5 but less than 3.0 cubic centimeters per minute.

Dielectric Liquid

During the development of the liquid-layer spark technique, the property that appeared to measure the effectiveness of the liquid layer was the dielectric breakdown strength. In some cases, the effectiveness has been related to the liquid dielectric constant. Prior to the analysis of superalloys, a study with liquid C_2 to C_8 alcohols and hydrocarbons compared the amount of sample removed to that observed in air and with a water layer.

Sample removal by alcohols was comparable to removal by water. Hydrocarbons were less effective then alcohols but more effective than that observed in air. The carbon compounds introduced significant cyanogen and carbon neutral atom and ion spectra; whereas, carbon species spectra were almost totally absent with the water layer. Emission from nitrogen ions was most effectively reduced by the water layer. Compared with sparking in air, oxygen ion emission was reduced with water and with carbon compounds and became more effectively reduced as the carbon number increased. This result might suggest the formation of carbon oxide species in the discharge.

A second experiment was conducted to examine compounds which could produce unique elemental emission that might be employed as a reference standard (i.e., liquid-layer internal standard). Although halogenated methane compounds produced chlorine ion emission, the spark crater was small and discolored, and emission intensity was low. A silicone fluid ($(SiO)_x$) gave results comparable to a water layer; however, nitrogen ion emission was strong. Silicon neutral atom and ion emissions were observed and could potentially serve as reference standards.

For the preliminary development of the spark spectroanalysis of superalloys, water and aqueous solutions were used in the liquid-layer spark technique. The use of other liquids is possible.

REFERENCES

1. Barnes, Ramon, M.: Application of Liquid-Layer Solid-Sample Spark Technique to Spectrochemical Spark Source. NASA TM X-1429, 1967.

2. Anon.: Methods for Emission Spectrochemical Analysis. Fourth ed., ASTM, 1964.

3. Freche, J. C.; Ashbrook, R. L.; and Sandrock, G. D.: High-Temperature, Cobalt-Tungsten Alloys for Aerospace Applications. J. Eng. Industry, vol. 87, no. 1, Feb. 1965, pp. 9-20.

4. Walters, J. P.: An Adjustable-Waveform High-Voltage Spark Source for Optical Emission Spectroscopy. Anal. Chem., vol. 40, no. 11, Sept. 1968, pp. 1672-1682.

NASA-Langley, 1969 —— 6 E-4778